Title

Inhibition of soluble epoxide hydrolase alleviated atherosclerosis by reducing monocyte infiltration in Ldlr−/− mice

Authors

Li, Dan
Liu, Yajin
Zhang, Xu
et al.

Publication Date

2016-09-01

DOI

10.1016/j.yjmcc.2016.08.001

Peer reviewed

HHS Public Access

Author manuscript

J Mol Cell Cardiol. Author manuscript; available in PMC 2017 September 01.

Published in final edited form as:

J Mol Cell Cardiol. 2016 September ; 98: 128–137. doi:10.1016/j.yjmcc.2016.08.001.

Inhibition of Soluble Epoxide Hydrolase Alleviated Atherosclerosis by Reducing Monocyte Infiltration in *Ldlr*$^{-/-}$ Mice

Dan Li[1,#], **Yajin Liu**[2,#], **Xu Zhang**[2], **Huizhen Lv**[2], **Wei Pang**[1], **Xiaoli Sun**[1], **Li-Ming Gan**[3], **Bruce D Hammock**[4], **Ding Ai**[2], and **Yi Zhu**[1,2,*]

[1]Department of Physiology and Pathophysiology, Peking University Health Science Center, Beijing, 100191, China

[2]Collaborative Innovation Center of Tianjin for Medical Epigenetics and Department of Physiology and Pathophysiology, Tianjin Medical University, Tianjin, 300070, China

[3]Innovative Medicines & Early Development, AstraZeneca R&D, SE-431 83 Mölndal, Sweden

[4]Department of Entomology and Nematology UC Davis Comprehensive Cancer Center, University of California, Davis, Davis, CA 95616, USA

Abstract

Rationale—Circulating monocytes play pivotal roles in chronic inflammatory diseases. Epoxyeicosatrienoic acids (EETs), metabolites of arachidonic acid, are known to have anti-inflammatory effects and are hydrolyzed by soluble epoxide hydrolase (sEH).

Objective—We aimed to investigate the effect of sEH inhibition in atherogenesis.

Methods and Results—Mice with low-density lipoprotein receptor deficiency (*Ldlr*$^{-/-}$) with or without sEH inhibitor, and *Ldlr/sEH* double-knockout (DK) mice were fed a Western-type diet (WTD) for 6 weeks to induce arteriosclerosis. Both sEH inhibition and gene depletion decreased the WTD–induced hyperlipidemia, plaque area and macrophage infiltration in mice arterial wall. Ly6C^{hi} infiltration of monocytes remained similar in blood, spleen and bone marrow of DK mice, but was decreased in aortic lesions. To further assess the role of sEH or EETs in monocyte/macrophage infiltration in atherogenesis, we transplanted DK bone marrow into *Ldlr*$^{-/-}$ recipients, and then fed mice the WTD. Aortic lesions and Ly6C^{hi} monocyte infiltration were reduced in mice with transplanted bone marrow of DK mice without diminishing the cholesterol level. Furthermore, sEH inhibition or gene depletion increased the ratio of EETs/DHETs and diminished the expression of P-selectin glycoprotein ligand 1 (PSGL-1) in mice peripheral-blood

*Correspondence: Yi Zhu, MD, Department of Physiology and Pathophysiology, Tianjin Medical University, Tianjin, 300070, China. Tel: (+86) 22-8333-6665; zhuyi@tmu.edu.cn.

#Both authors contributed equally to this work.

Disclosure of Conflicts of Interest

B.D.H. is an author of University of California patents on the synthesis and use of sEH inhibitors. These patents are licensed to EicOsis LLC. The other authors declare no competing financial interests.

mononuclear cells. Monocyte adhesion to P-selectin and to tumor necrosis factor α–activated endothelial cells was also diminished by sEH inhibition.

Conclusion—sEH inhibition and gene depletion attenuated atherosclerosis in mice by decreasing the infiltration of monocytes into the artery wall. EET and PSGL-1 may play pivotal roles in monocyte/macrophage infiltration and atherogenesis.

Keywords

soluble epoxide hydrolase; epoxyeicosatrienoic acids; atherosclerosis; inflammation; monocyte; macrophage; P-selectin glycoprotein ligand-1

Introduction

Atherosclerosis is a chronic inflammatory disease characterized by dyslipidemia, foam cell formation and lipid plaque accumulation in the artery wall. The process of circulating monocyte/macrophage adhesion on the endothelium, infiltration into the sub-endothelial space and localization in the artery wall is the initial step of plaque formation. Hence, dysfunctional monocytes/macrophages play a pivotal role in atherogenesis.[1]

Blood monocytes in mice are mainly in two subsets, Ly6C^{lo} and Ly6C^{hi} subsets; the latter is considered the inflammatory and home to inflamed tissues. These inflammation-related monocytes release proinflammatory cytokines to cause inflammation and immune responses.[2,3] The Ly6C^{hi} subset is newly released from bone marrow and then mature in circulating blood.[4] Inflammatory stimulation increases the number of Ly6C^{hi} monocytes in blood. P-selectin glycoprotein ligand-1 (PSGL-1), a transmembrane glycoprotein in leukocytes, interacts with 3 selectins, namely, P-selectin, E-selectin and L-selectin.[5] PSGL-1 is expressed on all leukocytes, including blood monocytes, especially the Ly6C^{hi} subset. When PSGL-1 on monocytes binds to the selectins on endothelial cells (ECs) surface in vasculature, atherogenesis is initiated.

Bioactive small-molecule lipid mediators regulate cell function. Regioisomers of epoxyeicosatrienoic acids (EETs), the metabolites of arachidonic acid, possess cardioprotective functions.[6] The enzyme soluble epoxide hydrolase (sEH) is expressed in various tissues and cells, including leucocytes.[7] The bioactivity of EETs is reduced by sEH if hydrolyzed to their corresponding dihydroxyeicosatrienoic acids (DHETs). Increasing EET level by sEH inhibition reduces hyperlipidemia, inflammation and causes vessel dilation; thus, sEH is a potential therapeutic target for cardiovascular diseases such as hypertension and atherosclerosis.[8–11] Previously studies reported that sEH inhibition could increase EET level and decrease angiotensin II-induced atherosclerotic plaque area in ApoE-null mice, but the plasma cholesterol-lowering effect of sEH inhibition was not consistent.[8,12] The mechanism underlying the inhibition of endothelial activation is down regulation of endothelial inflammatory markers, i.e. intercellular adhesion molecule-1. However, the mechanism of sEH inhibition and increased EET level on monocyte/macrophage infiltration in atherogenesis still remains unclear.

To elucidate the underlying mechanism of atherosclerosis, we explore the role of monocytes/macrophages by sEH inhibition or gene deletion in low-density lipoprotein receptor deletion (*Ldlr*$^{-/-}$) mice. *Ldlr*$^{-/-}$ mice with sEH inhibition treatment and *Ldlr/sEH* double-knockout (DK) mice were used. To exclude the lipid-lowering effect of sEH inhibition in vivo, we also used transplantation of bone marrow of DK mice. sEH inhibition decreased the expression of PSGL-1 in monocytes and restrained the infiltration of Ly6C^{hi} monocytes into the artery wall, consequently suppressed the inflammatory response and plaque formation in the early stage of atherosclerosis in *Ldlr*$^{-/-}$ mice.

Materials and Methods

Cell isolation and culture

Human umbilical vein endothelial cells (HUVECs) were cultured as described.[13, 14] Peripheral blood from *Ldlr*$^{-/-}$ and DK mice was collected and diluted with phosphate buffered saline (PBS). To gain more mononuclear cells, spleens were isolated from *Ldlr*$^{-/-}$ and DK mice and then smashed, and cells were passed through a 200-mesh screen. The diluted solution was centrifuged and re-suspended with PBS at 1:1. The diluted samples underwent density gradient separation on Ficol-Paque Plus (GE Healthcare Life Sciences, Buckinghamshire, UK) at 1:1 and were centrifuged. Then, the layer of peripheral blood mononuclear cells (PBMCs) was collected and re-suspended with red blood cell lysis buffer to delete the red blood cells, then washed twice with PBS. The isolated mononuclear cells were used for further experiments.

Flow cytometry

Splenic mononuclear cells of *Ldlr*$^{-/-}$ or DK mice were treated with or without 1 μM *trans*-4-{4-[3-(4-trifluoromethoxyphenyl)-ureido] cyclohexyloxy} benzoic acid (*t*-TUCB), an sEH inhibitor, and 1 μM 14,15-EET (Cayman Chemical; Ann Arbor, MI) for 12 h. After washing, 1×10^6 cells were stained for 30 min on ice with anti-mouse PE anti-mouse PSGL-1 (BD Pharmingen, San Jose, CA). Harvested aortas from *Ldlr*$^{-/-}$ and DK mice fed with WTD were microdissected and digested with 125 U/ml collagenase type XI, 60 U/ml hyaluronidase type I, 60 U/ml DNase1, and 450 U/ml collagenase type I (all enzymes were obtained from Sigma-Aldrich) in PBS containing 20 mM HEPES at 37°C for 1 h. A cell suspension was obtained by mashing the aorta through a 70-μm strainer. Cells were incubated with FITC-CD45, anti-mouse PE-CD11b and anti-mouse APC-Ly6C (Biolegend, San Diego, CA) for 20 min at 4°C, washed twice, and incubated with secondary Abs for an additional 20 min. Flow cytometry was involved in the use of FACS Calibur (Becton Dickinson, San Jose, CA) and data were analyzed by use of FlowJo (Tree Star, Ashland, OR).

Adhesion assay under static conditions

PBMC adhesion to ECs was measured as described.[15] Briefly, HUVECs were incubated with M199 (Gibco, Grand Island, NE) containing 10% fetal bovine serum (FBS; Hyclone/Thermo Scientific, Waltham, MA) with or without recombinant human tumor necrosis factor α (TNFα, 10 ng/ml, Peprotech, Rocky Hill, NJ) for 4 h. In some treatment groups, the endothelial monolayer was preincubated with blocking antibodies for E-selectin or P-

selectin (10 μg/mL, Biolegend, San Jose, CA) for 15 min at 37°C. At the end of incubation, the culture supernatant was removed and cells were washed 3 times with M199. PBMCs from *Ldlr*$^{-/-}$ or DK mice were treated with or without 1 μM *t*-TUCB and 1 μM 14,15-EET for 6 h. Fluorescently labeled PBMCs (BCECF-AM, Invitrogen, Carlabad, CA) were incubated with HUVECs at 37°C for 1 h. After washing, PBMC adhesion to HUVECs was quantified by measuring fluorescent cells in areas of 5 independent images per condition. The graph depicts the mean of 3 independent experiments.

Adhesion assay under flow conditions

PBMCs were preconditioned with or without 1 μM *t*-TUCB and 1 μM 14, 15-EET for 6 h. Vena8 biochips (Cellix, Dublin, Ireland) were pre-coated with 10 μg/ml recombinant mouse P-selectin (R&D system, Minneapolis, MN) at 37°C in a 5% CO_2 atmosphere for 30 min. Then, the biochip channels were superfused with suspensions of 3×10^6/ml PBMCs from mice at 0.5 dyne/cm^2 for 2 min. Cell adhesion was monitored with an inverted microscope and digital camera with VenaFlux software (Cellix). Computerized image analysis involved use of Image J, with adherent cells quantified on each single image. At each shear stress value, at least 5 fields of view of cell rolling and adhesion were calculated along the length of the channel.[16]

Real-time PCR analysis

Total RNA from cells or the aortic arch in mice was isolated with use of Trizol reagent (Transgen Biotech, Beijing, China) and reverse-transcribed by use of the first-strand cDNA synthesis kit (Thermo Scientific, Rockford, IL). Gene expression was normalized to that of β-actin. The primers were for *Mcp1*: 5′-AGGTCCCTGTCATGCTTCTG-3′ (F) and 5′-TCTGGACCCATTCCTTCTTG-3′ (R); *Tnfa*: 5′-CCAGACCCTCACACTCAGATC-3′ (F), 5′-CACTTGGTGGTTTGCTACGAC-3′ (R)*; Il-1β*: 5′-GCCCATCCTCTGTGACTCAT-3′ (F), 5′-AGGCCACAGGTATTTTGTCG-3′; *Cd68*: 5′-CCCAAGGAACAGAGGAAG-3′ (F) and 5′-GTGGCAGGGTTATGAGTG-3′ (R)*; F4/80*: 5′-CTTTGGCTATGGGCTTCCAGTC-3′ (F) and 5′-GCAAGGAGGACAGAGTTTATCGTG-3′ (R); *Psgl-1*: 5′-GGTGGTTGGGGATGACGATT-3′ (F) and 5′-TGGACGGTCTCTACTGAGGT-3′ (R); *β-actin*: 5′-ATCTGGCACCACACCTTC-3′ (F), 5′-AGCCAGGTCCAGACGCA-3′ (R).

Metabolomic analysis

Metabolomic analysis by LC-MS/MS for EETs and DHETs was performed as we previously described.[17,18] Briefly, samples of mice serum were homogenized with 500 μl methanol with 2% formic acid and 0.01 mol/L BHT, extracted by solid-phase extraction and spiked with internal standard mixture (5 ng). Then, cartridges were washed with 1 ml of 5% methanol and pumped vacuum. Analytes were eluted with methanol and evaporated to dry. The residues were dissolved in 100 μl of 30% acetonitrile. Samples of 1×10^7 splenic mononuclear cells were homogenized with 500 μl methanol, spiked with isotopic internal standard mixture. Samples were mixed on a vortexer for 5 min. After centrifugation (12000 g for 10 min at 4°C), the supernatant was transfered into a new tube. 700 μL water and 1 ml ethyl acetate were added to the supernatant. The sample were mixed vigorously for 2 min and centrifuged for 10 min at 12000 g. The upper organic phase was transferred into a new

tube and the water phase was extracted for another time. The organic phase was combined and then evaporated to dryness. Chromatographic separations involved use of an UPLC BEH C18 column (1.7 μm, 100 × 2.1 mm i.d.) consisting of ethylene-bridged hybrid particles (Waters, Milford, MA). Target profiling of EETs and DHETs was detected by use of the 5500 QTRAP hybrid triple quadrupole linear ion-trap mass spectrometer (AB Sciex, Foster City, CA) equipped with a turbo ion-spray electrospray ionization source.

Animal experiments and sample collections

All animal experiments were approved by the Institutional Animal Care and Use Committee of Peking University Health Science Center. All mice were maintained under controlled temperature and a 12-h light/dark cycle with free access to water and standard diet. *sEH*$^{-/-}$ mice were cross-bred with *Ldlr*$^{-/-}$ C57BL/6 mice to obtain DK mice. Eight-week-old male *Ldlr*$^{-/-}$ and their littermate DK mice (n=12 each group) were fed chow (Research Diets, Inc. D12102 containing 10 kcal% fat) or a Western-type diet (WTD, Research Diets, Inc. D12109 containing 40 kcal% fat, 1.25% cholesterol, 0.5% cholic acid) for 6 weeks. One group of *Ldlr*$^{-/-}$ mice was fed a WTD plus the sEH inhibitor *t*-TUCB (20 mg in 5 ml PEG400, then dissolved in 1 L drinking water). After feeding, plasma samples were collected in heparin for an anticoagulant. The plasma concentrations of triglycerides, total cholesterol, LDL-C and HDL-C in mice were measured by use of an automated clinical chemistry analyzer kit (Biosino Biotech, Beijing, China).

Aortic trees were obtained and fixed in 4% paraformaldehyde solution for *en face* staining. Aorta samples for RT-PCR were snap-frozen in liquid nitrogen immediately after collection and then stored at −80°C. Samples of aortic roots were embedded in Tissue-Tec OCT molds at −40°C after fixing and dehydrating.

Bone marrow transplantation

Recipient female *Ldlr*$^{-/-}$ mice were given 100 mg/L neomycin and 10 mg/L polymyxin B in acidic drinking water both 1 week before and 2 weeks after irradiation with 900 rads by using a cesium gamma source in Peking University. At 4 h after irradiation, recipient female mice were injected with bone marrow cells. The femurs of male *Ldlr*$^{-/-}$ and DK mice were flushed with medium containing RPMI 1640, 2% FBS, heparin and penicillin to obtain bone marrow cells. Cells were washed twice with serum-free RPMI 1640 and centrifuged at 2000 rpm for 5 min at 4°C, counted, and suspended at 1×10^7 cells/ml; 0.5 ml cells was injected by tail vein in each recipient mouse. After 8 weeks of transplantation, mice were fed a WTD.

Histopathological assessments

Aortic trees were fixed and dissected on dark wax, then stained with Oil-red O to quantify the lesion area by use of Image J. Cross sections of aortic roots at 7 μm thickness were stained with Oil-red O to assess lipid accumulation. To calculate the lesion area in aortic roots, outflow tract sections were stained with hematoxylin and eosin. Immunohistochemical staining with the primary antibody anti-Mac-3 (1:100, Santa Cruz Biotechnology, Santa Cruz, CA) was used to evaluate macrophage infiltration in aortic roots. Collagen formation was detected by 0.1% picrosirius red staining (Fluka, Germany).

Monocyte infiltration experiment

To track newly infiltrated monocytes in aortic plaque, the Ly6C^{hi} monocyte subset was labeled with fluorescent microspheres as described previously.[19] Briefly, mice with bone marrow transplantation were injected intravenously with 250 μl clodronate-containing liposomes to deplete monocytes 4 days before a 6-week WTD in *Ldlr*$^{-/-}$ female mice. Two days later, the mice were injected with Fluoresbrite Plain YG microspheres (Polysciences) 1 μm in diameter to label the newly generated Ly6C^{hi} monocytes. At the end of the experiment, aortas of mice were excised and newly recruited bead-labeled monocytes in atherosclerotic lesions were visualized by fluorescence microscopy and quantified by using Image J.

Statistical analysis

Data are expressed as mean ± SEM. Data were analyzed by the unpaired Student's *t* test or by one-way ANOVA with Bonferroni post-hoc test with GraphPad Prism software. Differences were considered significant at $p<0.05$.

Results

sEH inhibition decreased WTD-induced hyperlipidemia and atherosclerosis

To explore the role of sEH in atherosclerosis, we treated *Ldlr*$^{-/-}$ mice with the sEH inhibitor and generate DK mice with cross-bred *sEH*$^{-/-}$ mice with *Ldlr*$^{-/-}$ mice. There is no difference of body weight and blood pressure of *Ldlr*$^{-/-}$ with chow diet, WTD and WTD plus sEHI (date not shown). We measured the mRNA of *sEH* in the whole aorta of the mice and found that the level of *sEH* was increased in aorta followed by WTD with or without sEH inhibitor in *Ldlr*$^{-/-}$ mice (date not shown). To evaluate the efficiency of sEH inhibitor and gene deletion, we explored EET and DHET activity in plasma of mice by a metabolomic technique.[17,18] WTD decreased the ratio of EETs/DHETs in *Ldlr*$^{-/-}$ mice, but sEH inhibitor increased the ratio of both 14,15-EET/DHET and 11,12-EET/DHET, hallmark of sEH activity (Fig. 1A). The ratio of EETs/DHETs was higher in mice with *sEH*$^{-/-}$ mice as compared to sEH inhibition with either diet. Plasma cholesterol levels and progression of atherosclerosis were evaluated after feeding mice with WTD for 6 weeks. Plasma levels of total cholesterol and low-density lipoprotein cholesterol (LDL-C) were increased in *Ldlr*$^{-/-}$ and DK mice on WTD, in which the level of high-density lipoprotein cholesterol (HDL-C) was decreased. Plasma total cholesterol, LDL-C and HDL-C levels were not changed in mice on chow diet. sEH inhibition and gene deletion reduced the levels of total cholesterol and LDL-C in plasma by about 20% (Fig. 1B). Atherosclerotic lesion area (Oil-red O–positive) was increased in aortas of *Ldlr*$^{-/-}$ mice, with no apparent lesions in the aortas of *Ldlr*$^{-/-}$ and DK mice on chow diet. Compared with the atherosclerotic lesion area in *Ldlr*$^{-/-}$ mice, sEH inhibition and gene deletion significantly diminished the lesion area in aorta (Fig. 1C, D).

sEH inhibition decreased WTD-induced lesion area, lipid accumulation, and collagen formation in aortic root

We analyzed lesion area, lipid accumulation, collagen formation and macrophage infiltration in the aortic root. As compared with *Ldlr*$^{-/-}$ mice on WTD diet, sEH inhibition and gene deletion reduced the WTD-induced plaque area in the aortic root (Fig. 2A) and significantly reduced lipid accumulation and collagen deposition in atherosclerotic lesions.

sEH inhibition decreased macrophage infiltration and the expression of inflammatory genes in the aorta

To analyze the inflammatory response in the aorta, we explored macrophage infiltration by measuring expressions of Mac-3 and measured the expression of macrophage markers *Cd68* and *F4/80* to indicate macrophage infiltration. Both sEH inhibition and gene deletion reduced Mac-3–positive macrophage infiltration in aortic roots (Fig. 2A, bottom panel) and the mRNA level of *Cd68* and *F4/80* in the whole aorta as compared with *Ldlr*$^{-/-}$ mice on a WTD diet (Fig. 2B). We measured the gene expression of the pro-inflammatory factors *Mcp1*, *Tnfα* and *Il-1β*. All pro-inflammatory factors were upregulated in aortas of *Ldlr*$^{-/-}$ mice, and sEH inhibition and gene deletion could attenuate the expression of *Mcp1*, *Tnfα* and *Il-1β* at mRNA level (Fig. 2C).

sEH deficiency with bone marrow transplantation diminished the lesion area but did not alter plasma lipid levels in *Ldlr*$^{-/-}$ mice

To investigate the role of sEH inhibition in atherogenesis via inhibiting pro-inflammatory reaction other than the effects of cholesterol lowering, we transplanted the bone marrow of *Ldlr*$^{-/-}$ and DK mice into *Ldlr*$^{-/-}$ mice. After 6 weeks of WTD feeding, total plasma cholesterol, LDL-C and HDL-C were not changed in mice on WTD with sEH deletion in bone marrow (Fig. 3A). However, mice with DK bone marrow showed less lesion area in the whole aorta and the aortic root (Fig. 3B, 3C). Furthermore, Mac3-positive macrophage infiltration was decreased in aortic roots of mice with DK bone marrow, with no change in lipid accumulation or collagen formation (Fig. 3D), which supported the hypothesis that sEH inhibition in bone marrow-derived monocytes/macrophages is atheroprotective.

sEH deficiency decreased the infiltration of Ly6C^{hi} monocytes in aortic roots

To study the effect of sEH inhibition on monocyte infiltration, we tracked the newly recruited Ly6C^{hi} monocyte subset with labeled fluorescent beads in aortic lesions. Mice were injected with liposomes containing clodronate to eliminate monocytes in the artery wall. Fluorescent microspheres were injected to label the newly generated Ly6C^{hi} monocytes for 2 days. The invading beads in the aorta sections were harvested. sEH inhibition reduced the number of Ly6C^{hi} monocytes infiltrating into the sub-endothelial space in aortic root sections (Fig. 4A). The isolated cells of aorta from *Ldlr*$^{-/-}$ and DK mice fed with 6-week WTD were digested and stained with CD45, CD11b and Ly6C, the CD45^{+}CD11b^{+}Ly6C^{hi} cells are diminished in DK mice detected by FACS (Fig. 4B).

sEH deficiency decreased the expression of PSGL-1 in mononuclear cells

PSGL-1, as the ligand of P-selectin on the endothelium, initiates the process of monocyte rolling and adhesion during atherogenesis. We investigated the effect of sEH activity on PSGL-1 expression in monocytes/macrophages. To gain more PBMCs, we isolated PBMCs from spleen and treated the cells with *t*-TUCB, 14,15-EET and *t*-TUCB plus 14,15-EET for 6 hours. The results showed that sEH inhibitor and EET alone and combination decreased *Psgl-1* at mRNA level. There is no difference among these treatments (Fig. 5A). We also observed a decrease in the expression of *Psgl-1* in $sEH^{-/-}$ mice compared to WT mice (Fig. 5B). Treatment with the sEH inhibitor and EET supplementation and combination could also downregulate *Psgl-1* at the mRNA level in cultured PBMCs from $Ldlr^{-/-}$ mice (Fig. 5C). The decrease in the expression of *Psgl-1* in DK mice was also observed (Fig. 5D). sEH inhibition with EET supplementation decreased PSGL-1 at the protein level as detected by flow cytometry of PBMCs (Fig. 5E).

sEH deficiency decreased the adhesion of PMBCs to P-selectin and on ECs

To study the effect of sEH inhibition on PBMCs function, we measured the rolling function of PBMCs on coated purified protein in the Cellix micro-flow system. PBMCs from $Ldlr^{-/-}$ mice were treated with the sEH inhibitor and 14,15-EET, and then loaded to the fluid channel on P-selectin coated biochip, with 0.5 dyne/cm^2 shear stress for 2 min. Cells from $Ldlr^{-/-}$ mice rolled slower and showed higher adhesion ability on P-selectin as compared with that from DK mice. Moreover, sEH inhibition and EET supplementation decreased PBMCs adhesion on P-selectin (Fig. 6A and 6B). PBMC originated from $Ldlr^{-/-}$ mice showed stronger adhesion on TNFα-activated ECs than those from DK mice. Both sEH inhibition and EET supplementation decreased PBMCs adhesion. Pre-treatment with neutral antibodies against P-selectin and E-selectin partially blocked PBMCs adherent to activated ECs (Fig. 6C and 6D).

Discussion

Hypercholesterolemia and monocyte/macrophage infiltration are pivotal in the initiation of atherogenesis. Bioactive metabolites of arachidonic acid as lipid mediators possess various functions regulating the cell and are involved in cardiovascular diseases.[6] sEH hydrolizes EETs to DHETs and reduces the cardioprotective effect of EETs. sEH inhibition with elevated levels of EETs are thought to lower hypercholesterolemia and reduce inflammation, which may attenuate atherosclerosis development and aneurysm formation.[8] Here, we investigated the role of sEH inhibition in atherogenesis and the underlying mechanism with a sEH chemical inhibitor and gene knockout in mice. We found that (1) *t*-TUCB, a potent sEH inhibitor, and gene deletion retarded hyperlipidemia and atherosclerotic lesion formation induced by a 6-week WTD in aortas of $Ldlr^{-/-}$ mice; (2) mice with sEH gene-deficient bone marrow transplantation did not show altered lipid values but did show reduced atherosclerosis; (3) sEH inhibition lessened $Ly6C^{hi}$ monocyte infiltration in aortic lesions; and (4) sEH inhibition and/or 14,15-EET supplement reduced the expression of PSGL-1 on monocytes and reduced its rolling and adhesion on the endothelium. This mechanism may provide a novel insight into targets in atherosclerosis.

sEH is distributed in many tissues and cells.[7] In normal animal, 90% of the metabolism of EETs is by sEH, β-oxidation, chain elongation, chain shortening, omega-1 hydroxylation and other pathways may also play a role on EET metabolism, especially when *sEH* gene is knockout.[6] Indeed, our results showed that the ratio of EETs/DHETs increased in DK mice, but they were slightly decreased with WTD, suggesting that without sEH, the rate of EET metabolism is only decreased but not eliminated. Inhibited sEH activity and elevated EET concentration have been described in many conditions associated with inflammation. Previously, we and other groups reported that sEH inhibition reduced hypertension, cardiac hypertrophy and fatty liver in mice.[10, 20, 21] As well, other sEH chemical inhibitors AR9276 and AEPU decreased angiotensin II-induced atherosclerosis in $ApoE^{-/-}$ mice, but AEPU did not affect blood cholesterol levels.[8, 12] We found that a more powerful urea-based sEH inhibitor, *t*-TUCB, could reduce hyperlipidemia and atherosclerotic lesion formation in aortas of $Ldlr^{-/-}$ mice. However, sEH gene-deficient bone marrow transplantation reduced atherosclerosis without affecting plasma cholesterol levels, which illustrates the plasma-lowering effect of sEH on atherogenesis. Gene knockout and inhibition of sEH also prevented vascular remodeling by proliferation of smooth muscle cells in an inflammatory model but not a blood-flow dependent model of neointima formation in $ApoE^{-/-}$ mice.[22] These findings support our results that sEH inhibition decreased the inflammation in the pathologic process of the artery wall. sEH inhibition was reported to ameliorate inflammatory diseases and macrophage invasion.[8] sEH inhibition reduced macrophage infiltration to relieve angiotensin-dependent renal damage and pathological remodeling after myocardial infarction in rats.[23] Here, we found that sEH inhibition reduced atherosclerosis induced by a WTD in mouse aortas by blocking monocyte/macrophage infiltration.

The amount of Mac-3–positive macrophages was reduced in aortic lesions of DK mice, so mice with sEH gene deficiency in bone marrow-derived cells showed decreased lesion area and less infiltration of the $Ly6C^{hi}$ subset of monocytes in the aortic root. During inflammation, monocytes and other leukocytes first tether to roll on the activated endothelial cells adhere to and then transmigrate to the vasculature wall. The initial steps are primarily mediated by selectins, including P-selectin, E-selectin and L-selectin, which all bind to their common ligand PSGL-1 on the surface of mononuclear cells. PSGL-1 is a transmembrane glycoprotein with extracellular, transmenbrane and cytoplasmic domains. The N-terminal region of PSGL-1 is important for binding to selectins.[24] The expression of PSGL-1 and degree of glycosylation differ in subtypes of leukocytes. These differences contribute to selective recruitment of different types of leukocytes to inflammatory tissues. Fully glycosylated PSGL-1 on TH1 or TH2 cells interact with P-selectin and E-selectin on endothelium, platelets or platelet-enriched microparticles, and then mediate the recruitment of these cells to aortic plaque.[25] Mast cells and neutrophils may also use PSGL-1 to home to aortic lesions.[26] The $Ly6C^{hi}$ monocyte subset is the inflammatory type of leukocytes and expresses a higher level of PSGL-1 to interact with selectins on endothelial cells or activated platelets adherent to arterial wall. We found that sEH inhibition reduced the expression of PSGL-1 on monocytes and reduced its rolling and adhesion on the endothelium and reduced atherosclerotic lesion area. Elucidating the role of monocytes in atherogenesis and the underlying mechanism controlling monocyte rolling and adhesion on the injured surface of the endothelium is critical for understanding the pathogenesis and progression of

atherosclerosis. We provide evidence that PSGL-1 plays an important role in chronic atherosclerotic lesion formation.

Our study contains some limitations. One is that we used loss-of-function animal models only without gain-of-function experiments. Also, we might have overexpressed sEH in monocytes and detected the rolling and adhering function, however, lower transfection efficiency in primary isolated monocytes prevented for this study. Finally, we did not illuminate the detailed regulatory mechanism of sEH inhibiting PSGL-1 expression. We previously reported that EET is the endogenous ligand of peroxisome proliferator-activated receptor γ (PPARγ) in ECs.[27] We treated PBMCs from WT mice with 14,15-EET to downregulate PSGL-1, Pre-treatment of GW9662, a PPARγ inhibitor, could not reverse the effect of EET and the treatment of rosiglitazone, a PPARγ agonist, did not significantly alter the expression of *Psgl1* in PBMCs (date not shown). BCL6 and RUNX1 were reported as a silencer to transcriptionally downregulate PSGL1 in T follicular helper cells and Kasumi-1 cells.[28,29] EET did not upregulate either BCL6 or RUNX1 in PBMCs. Besides, EET treatment did not change the expression level of PPARγ. A systematic screening of the mechanism for the downregulation of PSGL1 by EETs may be needed in the future.

In conclusion, we provide evidence that monocytes with sEH inhibition or gene deletion ameliorated atherosclerosis induced by a WTD in $Ldlr^{-/-}$ mice by reducing the expression and function of PSGL-1. This finding may be experimental evidence that sEH inhibition is a promising target for atherosclerosis not only for cholesterol lowering but also for inhibiting monocyte/macrophage infiltration.

Acknowledgments

We acknowledge the Ministry of Science and Technology of China (2012CB517500), National Natural Science Foundation of China (81420108003, 81130002, 81470556), Collaborative Grant and NIEHS RO1 ES002710 and Superfund P42 ES004699 for financial support. Partial support was also provided by a Peking University-AstraZeneca Collaborative grant.

Abbreviations

sEH	Souble epoxide hydrolase
ARA	Arachidonic acid
HUVEC	Human umbilical vein endothelial cell
EET	Epoxyeicosatrienoic acid
PSGL-1	P-selectin glycoprotein ligand-1
MCP-1	Monocyte chemotactic protein-1
PBMC	Peripheral blood mononuclear cell
WTD	Western-type diet
PPARγ	Peroxisome proliferator-activated receptor γ

References

1. Hilgendorf I, Swirski FK, Robbins CS. Monocyte fate in atherosclerosis. Arterioscler Thromb Vas Biol. 2015; 35:272–9.
2. Libby P, Nahrendorf M, Swirski FK. Monocyte heterogeneity in cardiovascular disease. Semin Immunopathol. 2013; 35:553–62. [PubMed: 23839097]
3. Hilgendorf I, Swirski FK. Making a difference: Monocyte heterogeneity in cardiovascular disease. Curr Atheroscler Rep. 2012; 14:450–9. [PubMed: 22847772]
4. Tsou CL, Peters W, Si Y, Slaymaker S, Aslanian AM, Weisberg SP, Mack M, Charo IF. Critical roles for CCR2 and MCP-3 in monocyte mobilization from bone marrow and recruitment to inflammatory sites. J Clin Invest. 2007; 117:902–9. [PubMed: 17364026]
5. McEver RP, Cummings RD. Role of PSGL-1 binding to selectins in leukocyte recruitment. J Clin Invest. 1997; 100:S97–103. [PubMed: 9413410]
6. Spector AA, Fang X, Snyder GD, Weintraub NL. Epoxyeicosatrienoic acids (EETs): Metabolism and biochemical function. Prog Lipid Res. 2004; 43:55–90. [PubMed: 14636671]
7. Harris TR, Hammock BD. Soluble epoxide hydrolase: Gene structure, expression and deletion. Gene. 2013; 526:61–74. [PubMed: 23701967]
8. Zhang LN, Vincelette J, Cheng Y, Mehra U, Chen D, Anandan SK, Gless R, Webb HK, Wang YX. Inhibition of soluble epoxide hydrolase attenuated atherosclerosis, abdominal aortic aneurysm formation, and dyslipidemia. Arterioscler Thromb Vas Biol. 2009; 29:1265–70.
9. Larsen BT, Miura H, Hatoum OA, Campbell WB, Hammock BD, Zeldin DC, Falck JR, Gutterman DD. Epoxyeicosatrienoic and dihydroxyeicosatrienoic acids dilate human coronary arterioles via bk(Ca) channels: Implications for soluble epoxide hydrolase inhibition. Am J Physiol Heart Circ Physiol. 2006; 290:H491–9. [PubMed: 16258029]
10. Imig JD, Zhao X, Capdevila JH, Morisseau C, Hammock BD. Soluble epoxide hydrolase inhibition lowers arterial blood pressure in angiotensin II hypertension. Hypertension. 2002; 39:690–4. [PubMed: 11882632]
11. Wang YX, Ulu A, Zhang LN, Hammock B. Soluble epoxide hydrolase in atherosclerosis. Curr Atheroscler Rep. 2010; 12:174–83. [PubMed: 20425256]
12. Ulu A, Davis BB, Tsai HJ, Kim IH, Morisseau C, Inceoglu B, Fiehn O, Hammock BD, Weiss RH. Soluble epoxide hydrolase inhibitors reduce the development of atherosclerosis in apolipoprotein e-knockout mouse model. J Cardiovasc Pharmacol. 2008; 52:314–23. [PubMed: 18791465]
13. Zhu Y, Liao H, Xie X, Yuan Y, Lee TS, Wang N, Wang X, Shyy JY, Stemerman MB. Oxidized ldl downregulates atp-binding cassette transporter-1 in human vascular endothelial cells via inhibiting liver x receptor (lxr). Cardiovasc Res. 2005; 68:425–32. [PubMed: 16099444]
14. Liu Y, Zhu Y, Rannou F, Lee TS, Formentin K, Zeng L, Yuan X, Wang N, Chien S, Forman BM, Shyy JY. Laminar flow activates peroxisome proliferator-activated receptor-gamma in vascular endothelial cells. Circulation. 2004; 110:1128–33. [PubMed: 15313948]
15. Morlino G, Barreiro O, Baixauli F, Robles-Valero J, Gonzalez-Granado JM, Villa-Bellosta R, Cuenca J, Sanchez-Sorzano CO, Veiga E, Martin-Cofreces NB, Sanchez-Madrid F. Miro-1 links mitochondria and microtubule dynein motors to control lymphocyte migration and polarity. Mol Cell Biol. 2014; 34:1412–26. [PubMed: 24492963]
16. Freeley M, O'Dowd F, Paul T, Kashanin D, Davies A, Kelleher D, Long A. L-plastin regulates polarization and migration in chemokine-stimulated human T lymphocytes. J Immunol. 2012; 188:6357–70. [PubMed: 22581862]
17. Li L, Li N, Pang W, Zhang X, Hammock BD, Ai D, Zhu Y. Opposite effects of gene deficiency and pharmacological inhibition of soluble epoxide hydrolase on cardiac fibrosis. PloS one. 2014; 9:e94092. [PubMed: 24718617]
18. Zhang X, Yang N, Ai D, Zhu Y. Systematic metabolomic analysis of eicosanoids after omega-3 polyunsaturated fatty acid supplementation by a highly specific liquid chromatography-tandem mass spectrometry-based method. J Proteome Res. 2015; 14:1843–53. [PubMed: 25736083]
19. Wang Y, Wang GZ, Rabinovitch PS, Tabas I. Macrophage mitochondrial oxidative stress promotes atherosclerosis and nuclear factor-kappab-mediated inflammation in macrophages. Circ Res. 2014; 114:421–33. [PubMed: 24297735]

20. Ai D, Pang W, Li N, Xu M, Jones PD, Yang J, Zhang Y, Chiamvimonvat N, Shyy JY, Hammock BD, Zhu Y. Soluble epoxide hydrolase plays an essential role in angiotensin II-induced cardiac hypertrophy. Proc Natl Acad Sci U S A. 2009; 106:564–9. [PubMed: 19126686]

21. Liu Y, Dang H, Li D, Pang W, Hammock BD, Zhu Y. Inhibition of soluble epoxide hydrolase attenuates high-fat-diet-induced hepatic steatosis by reduced systemic inflammatory status in mice. PloS one. 2012; 7:e39165. [PubMed: 22720061]

22. Revermann M, Schloss M, Barbosa-Sicard E, Mieth A, Liebner S, Morisseau C, Geisslinger G, Schermuly RT, Fleming I, Hammock BD, Brandes RP. Soluble epoxide hydrolase deficiency attenuates neointima formation in the femoral cuff model of hyperlipidemic mice. Arterioscler Thromb Vas Biol. 2010; 30:909–14.

23. Imig JD, Zhao X, Zaharis CZ, Olearczyk JJ, Pollock DM, Newman JW, Kim IH, Watanabe T, Hammock BD. An orally active epoxide hydrolase inhibitor lowers blood pressure and provides renal protection in salt-sensitive hypertension. Hypertension. 2005; 46:975–81. [PubMed: 16157792]

24. Huo Y, Xia L. P-selectin glycoprotein ligand-1 plays a crucial role in the selective recruitment of leukocytes into the atherosclerotic arterial wall. Trends Cardiovasc Med. 2009; 19:140–5. [PubMed: 19818951]

25. Mangan PR, O'Quinn D, Harrington L, Bonder CS, Kubes P, Kucik DF, Bullard DC, Weaver CT. Both Th1 and Th2 cells require P-selectin glycoprotein ligand-1 for optimal rolling on inflamed endothelium. Am J Pathol. 2005; 167:1661–75. [PubMed: 16314478]

26. Steegmaier M, Blanks JE, Borges E, Vestweber D. P-selectin glycoprotein ligand-1 mediates rolling of mouse bone marrow-derived mast cells on p-selectin but not efficiently on E-selectin. Eur J Immunol. 1997; 27:1339–45. [PubMed: 9209482]

27. Liu Y, Zhang Y, Schmelzer K, Lee TS, Fang X, Zhu Y, Spector AA, Gill S, Morisseau C, Hammock BD, Shyy JY. The antiinflammatory effect of laminar flow: the role of PPARgamma, epoxyeicosatrienoic acids, and soluble epoxide hydrolase. Proc Nati Acad Sci USA. 2005; 102:16747–52.

28. Poholek AC, Hansen K, Hernandez SG, Eto D, Chandele A, Weinstein JS, Dong X, Kaech SM, Dent AL, Crotty S, Craft J. In vivo regulation of Bcl6 and T follicular helper cell development. J Immunol. 2010; 185:313–26. [PubMed: 20519643]

29. Ponnusamy K, Kohrs N, Ptasinska A, Assi SA, Herold T, Hiddemann W, Lausen J, Bonifer C, Henschler R, Wishmann C. RUNX1/ETO blocks seletin-mediated adhesion via epigenetic silencing of PSGL-1. Oncegenesis. 2015; 4:e146.

Highlight

1. The inhibition of and knockout soluble epoxide hydrolase ameliorated the lesion of atherosclerosis in *Ldlr*$^{-/-}$ mice.
2. The mechanism of monocyte with soluble epoxide hydrolase deficiency in adhesion to aortic lesion is proposed.
3. The sEH inhibition of soluble epoxide hydrolase increased the ratio of EETs/DHETs and diminished the expression of P-selectin glycoprotein ligand 1 in monocyte from the mice.

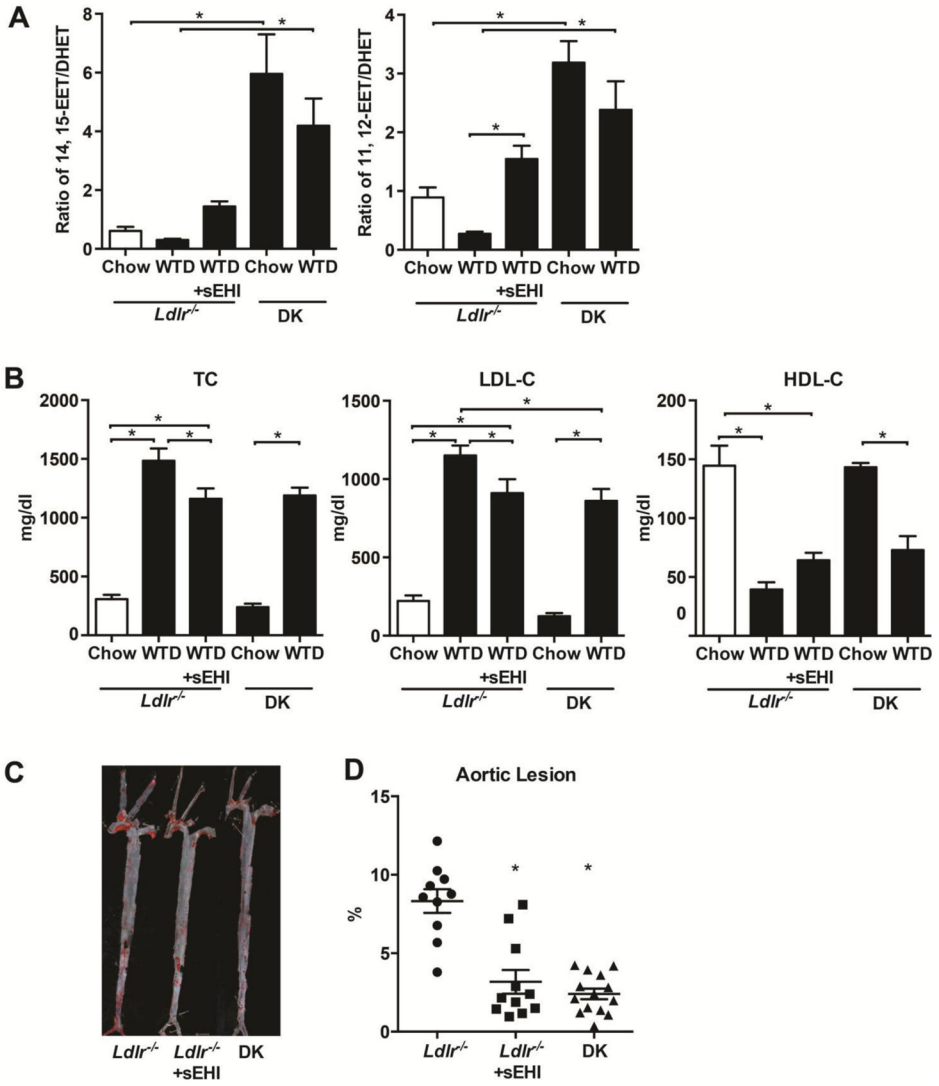

Figure 1. sEH inhibition decreased plasma levels of cholesterol and atherosclerotic lesions in *Ldlr*$^{-/-}$ mice

After *Ldlr*$^{-/-}$ and DK mice were fed chow or a WTD for 6 weeks, one group of *Ldlr*$^{-/-}$ mice were fed the WTD plus the sEH inhibitor *t*-TUCB (sEHI). (A) LC-MS/MS detection of the plasma ratios of 14,15-EET/DHET and 11,12-EET/DHET. (B) Quantification of plasma levels of total cholesterol, LDL-C and HDL-C in mice. (C) Representative aortas with Oil-red O staining and (D) Quantification of aortic lesion area from different mice (n≥10). Each dot represents a single male mouse. Horizontal bars represent mean values. Data are mean ±SEM, *p<0.05.

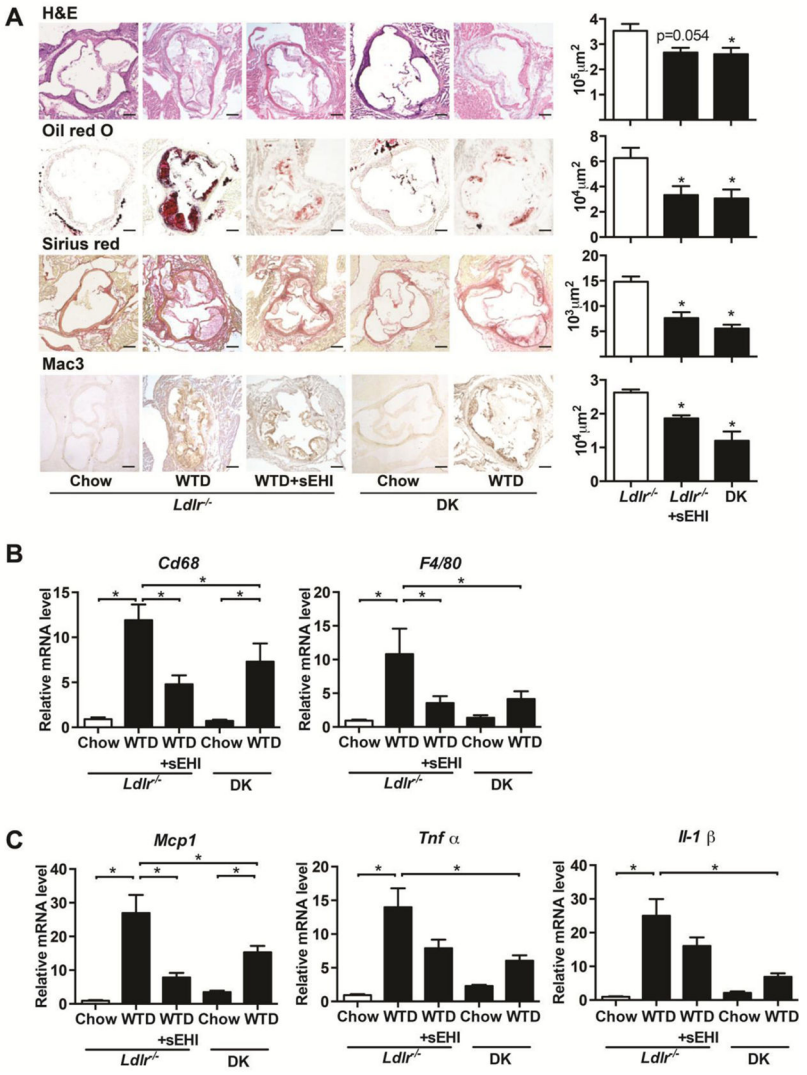

Figure 2. sEH inhibition reduced collagen formation, macrophage infiltration and the expression of proinflammatory genes in aortic arch of mice

Mice were treated as in Figure 1, (A) and cross sections of aortic roots were stained with H&E, Oil-red O, picrosirius red or immunostained with Mac-3. Quantification of positive areas of aortic roots on the right (n≥4). Scale bars, 200μm. (B) RT-PCR analysis of the mRNA levels of macrophage markers *Cd68* and *F4/80* (C) and markers of inflammatory status of vasculature *Mcp-1*, *Tnfα*, *Il-1β* (n≥8) in the aortic arch. Data are mean ±SEM, *p<0.05 vs. $Ldlr^{-/-}$ mice on WTD in A, B.

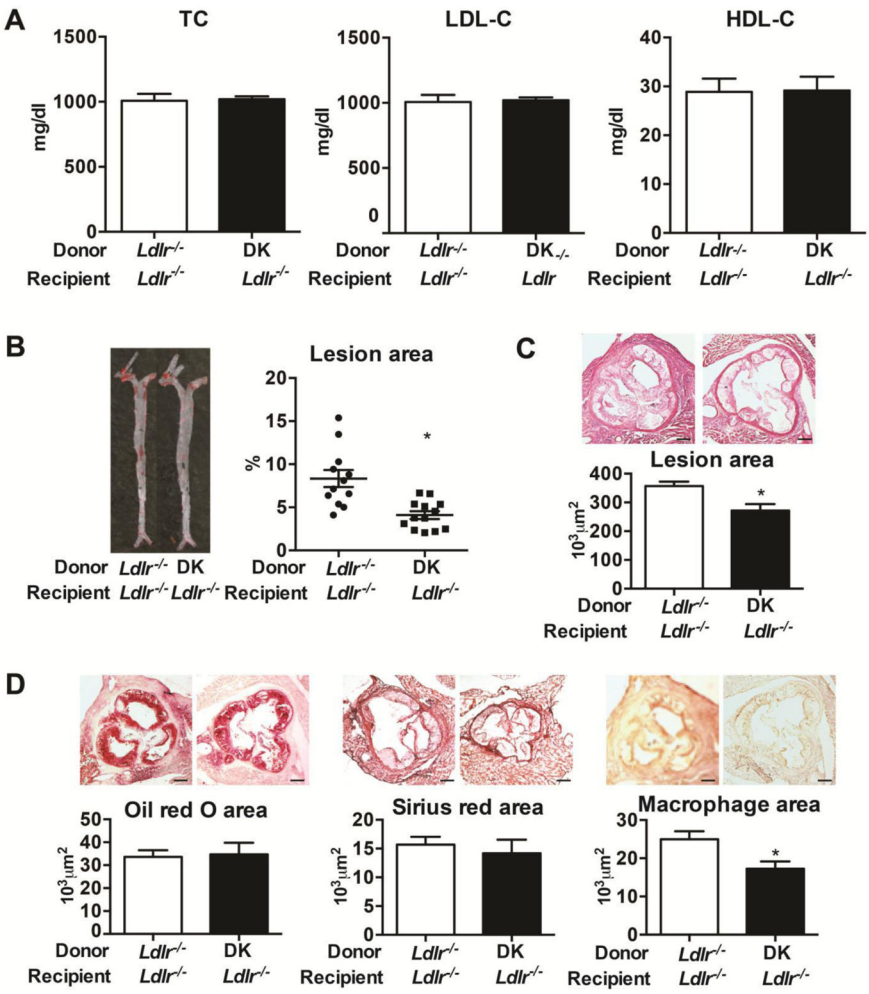

Figure 3. sEH gene deleletion of bone marrow transplantation diminished lesion area but did not alter the plasma levels of cholesterol in *Ldlr*$^{-/-}$ mice

After 8 weeks of bone marrow transplantation, mice were fed a WTD for 6 weeks. (A) Quantification of plasma concentrations of total cholesterol, LDL-C and HDL-C in plasma and (B) proportion of aortic lesion area (n≥10). Each dot represents a single mouse. Horizontal bars represent mean values. Whiskers are SEM. (C) Cross sections of aortic roots stained with H&E (n≥5). Scale bars, 200μm. (D) Representative photographs of Oil-red O, pircrosirius red and Mac-3 staining and quantification of positive staining area in aortic roots (n≥5). Scale bars, 200μm. Data are mean ±SEM, *p<0.05.

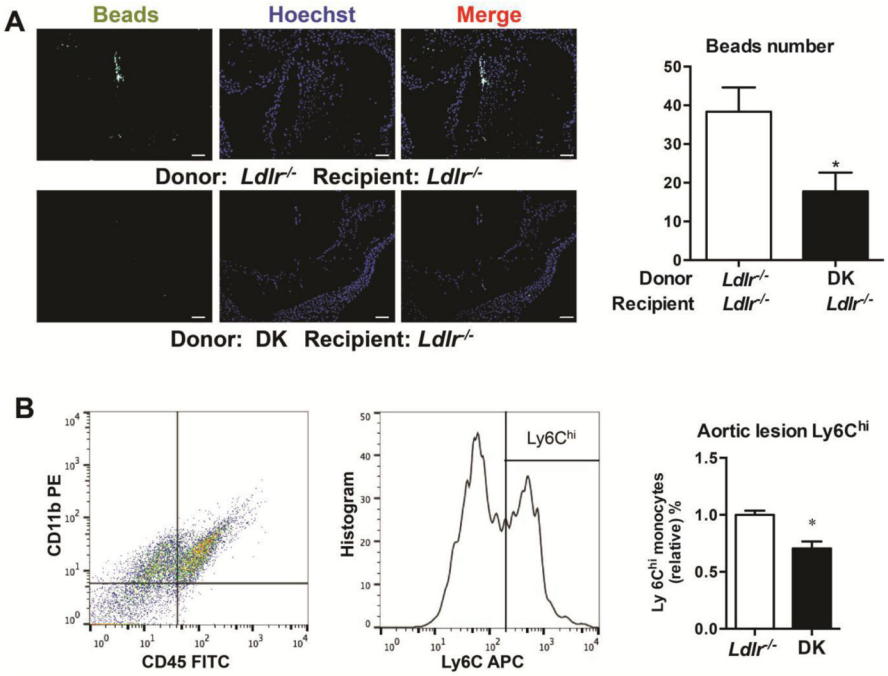

Figure 4. sEH deficiency decreased infiltration of Ly6C^{hi} subset of infiltration in aortic root

Mice with bone marrow transplantation were injected intravenously with 250 ml clodronate-containing liposomes for 2 days, then mice were injected with Fluoresbrite Plain YG microspheres (Polysciences), 1 mm in diameter, to label the newly-generated Ly6C^{hi} monocyte subset. After a 6-week WTD, aortas of *Ldlr*$^{-/-}$ female mice were excised and invading beads in aorta sections were quantified. (A) Representative fluorescence-labeled Ly6C^{hi} monocytes in aortic roots. Scale bars, 100μm. Quantification of bead number is on the right. n≥10, (B) The isolated cells of aorta from *Ldlr*$^{-/-}$ and DK mice fed with 6-week WTD were digested and stained by CD45, CD11b and Ly6C. The CD45^{+}CD11b^{+}Ly6C^{hi} cells were quantified. n=7. Data are mean ±SEM. *p<0.05.

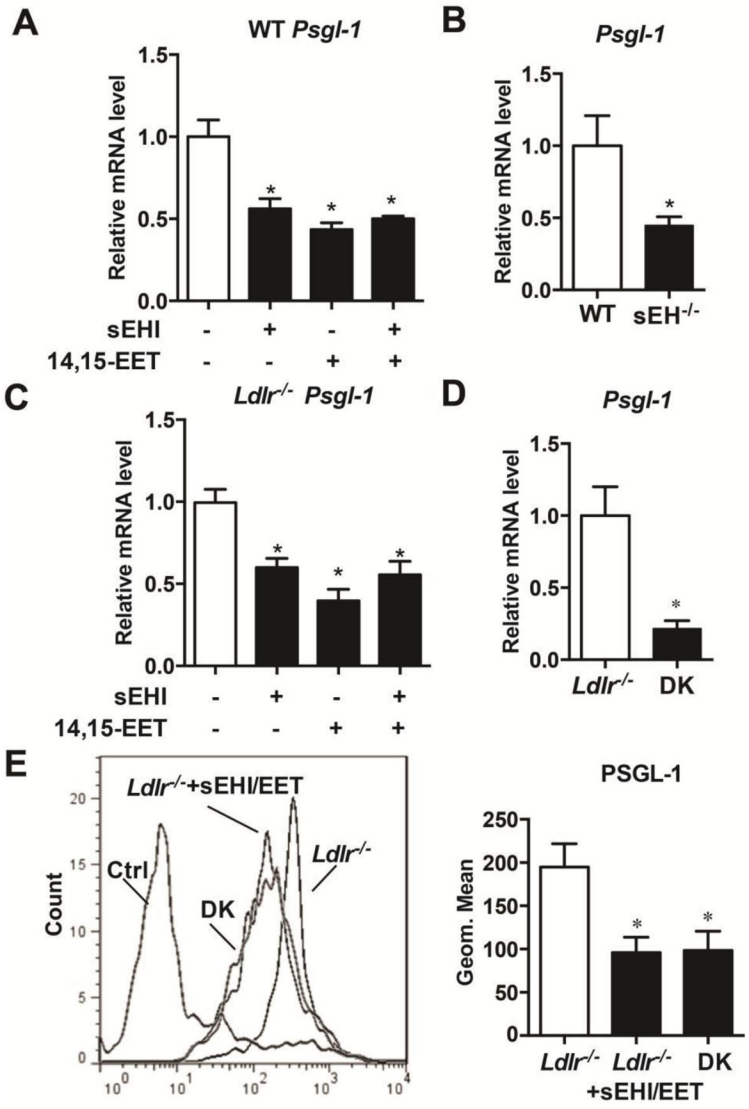

Figure 5. sEH deficiency decreased the expression of PSGL-1 in PBMCs

(A) RT-PCR analysis of the mRNA level of *Psgl-1* in splenic PBMCs from wild type mice and treated with sEHI (1 mM) and/or 14,15-EET (1 mM) (n=3). (B) RT-PCR analysis of the mRNA level of *Psgl-1* from blood PBMC in WT and $sEH^{-/-}$ mice (n≥9 per group). (C) RT-PCR analysis of the mRNA level of *Psgl-1* in splenic PBMCs from wild type and treated with sEHI (1 mM) and/or 14,15-EET (1 mM) (n=3). (D) RT-PCR analysis of the mRNA level of *Psgl-1* from blood PBMC in $Ldlr^{-/-}$ and littermates DK mice (n≥9 per group). (E) Flow cytometry of the expression of PSGL-1 in splenic PBMCs from $Ldlr^{-/-}$ mice treated without or with sEH inhibitor plus 14,15-EET for 12 h and PBMCs from DK mice and quantification (n≥10 per group). Data are mean±SEM.

*p<0.05.

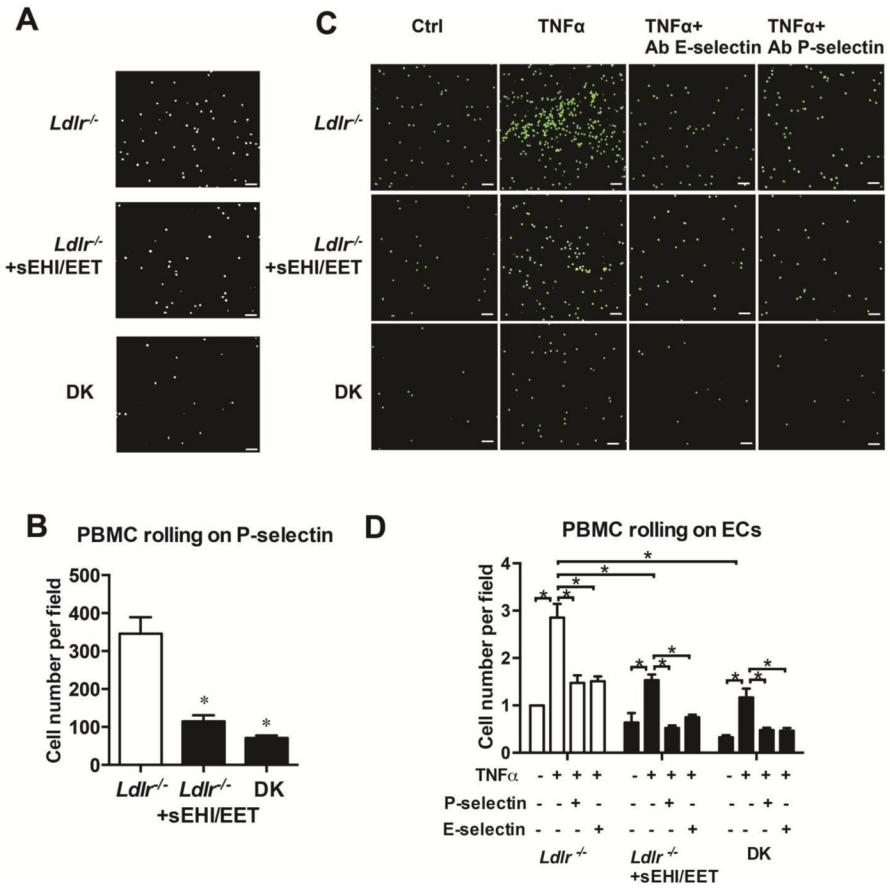

Figure 6. sEH inhibition or gene deletion decreases the adhesion of PMBCs on endothelial cells (ECs) and was selectin-dependent

(**A, B**) PBMCs isolated from *Ldlr*$^{-/-}$ mice treated with or without *t*-TUCB (1 m M) and 14,15-EET (1 m M) and DK mice for 6 h. Vena8 biochips were pre-coated with recombinant mouse P-selectin (10 mg/ml) for 30 min. Then, biochip channels were superfused with suspensions of 3×10^6/ml PBMCs at 0.5 dyne/cm^2 for 2 min. Cell adhesion was monitored with an inverted microscope and digital camera with VenaFlux software. Scale bars, 100μm. (**A**) Representative photographs of adhesion of PBMCs (200 x) and (**B**) quantification of cell numbers. (**C, D**) BCEDFAM labeled PBMCs from mice treated without or with sEH inhibitor (1 mM) and 14,15-EET (1 mM) and DK mice. Human umbilical vein ECs (HUVECs) were pretreated with TNFα for 6 h, then with anti-CD62P (for P-selectin) or anti- CD62E (for E-selectin) neutralized antibodies. (**C**) Representative photographs of adhesion of PBMCs on treated HUVECs and (**D**) quantification of cell numbers. 3 independent experiments. 3 *Ldlr*$^{-/-}$ and 3 littermate DK mice were used in each experiment. Data are mean ±SEM. *p<0.05 (two-way ANOVA).